Application of Model Predictive Control to the reactive extrusion of ϵ-Caprolactone in a twin-screw extruder ⋆

Maximilian Cegla [*,**] **Sebastian Engell** [*]

[*] *TU Dortmund University, Department of Biochemical and Chemical Engineering, Process Dynamics and Operations Group, Emil-Figge-Straße 70 44227 Dortmund , Germany*
[**] *Corresponding author: Maximilian Cegla (E-mail: maximilian.cegla@tu-dortmund.de)*

Abstract:
In this work the control of the reactive extrusion of ϵ-Caprolactone in a twin-screw extruder using nonlinear model predictive control with a tracking objective is investigated. For this, the modeling of the extrusion process using a one-dimensional mechanistic model is presented and extended to reactive extrusion systems. A novel modeling approach describing the pressure as a differential state is proposed to be able to use efficient optimization methods. Results for two scenarios, a change of the product quality and a change of the throughput are shown. The tuning of the controller is discussed and the benefits over traditional control methods are elaborated.

Keywords: Chemical engineering; Model predictive and optimization-based control; Hybrid and switched systems modeling; Reactive Extrusion; Polymerization; Twin-Screw Extrusion.

1. INTRODUCTION

The development of new polymers and the demand for a flexible and resource efficient production of these polymers are drivers for new processing technologies. Among the emerging technologies, the continuous production of polymers in a twin-screw extruder promises many benefits. This processing method offers a high flexibility in throughput and reactor design that regular reactors cannot offer. The combination of polymer synthesis and polymer processing leads to an energy and space-time efficient production. Furthermore, due to the possibility of using high mechanical energy, the twin-screw extruder is able to process solvent free high molecular weight polymers with high viscosity. Modeling of twin-screw extrusion processes leads to complex models of the internal flows as well of the reaction system. The complexity of the model is a consequence of the switching within the model between the cases of not entirely filled elements and filled elements in which pressure is built up that creates a pressure driven internal flow. The complexity of the process motivates the application of advanced process control strategies using the knowledge of the internal physical relations to drive the process to the desired set-point. Previous works of Grimard et al. (2016) showed the general applicability of MPC to control twin-screw extruders and focused on the description of the strong non-linearity of the system that is already present with a very general extruder model. In this work, we use a more refined extruder model that can easily be tailored to various setups of the reactive extruder. Model predictive control is applied to the ring opening polymerization of ϵ-Caprolactone which is a biodegradable polyester that is used in the production of polyurethanes and for drug delivery in the pharmaceutical industry. This system is a widely investigated reaction system and therefore data of the rheological behavior and the reaction system is available. First the reader is introduced to the general modeling methodology used to describe twin-screw extruders and the necessary extension to describe the reactive system of ϵ-Caprolactone. Then the control problems for two situations of changes in the product quality and of the throughput are presented and the results are discussed in detail.

⋆ The project leading to this publication has received funding from the European Union's Horizon 2020 research and innovation programme under grant agreement No 820716 (SIMPLIFY). (www.spire2030.eu/simplify)

2. MODELING

2.1 General model

A co-rotating twin-screw extruder consists of two rotating screws that are transporting material. The material leaves the extruder through a die that generates a pressure increase due to its small diameter. The screws are surrounded by barrel elements that can be heated by an electrical heating or cooled by cooling water. For modeling, the free space between the screws and the barrel is discretized into finite volumes of length Δx indexed by i as shown in Fig. 1. Between these elements material flow is generated by two mass transport phenomena: a conveying flow pushing material either forward ($m_{f,i}$) or backward ($m_{b,i}$) and a pressure driven flow $m_{p,i}$. The conveying flow $m_{c,i}$ depends on the rotation speed of the screws n, the local filling ratiof_i, the density ρ_i, the screw diameter D and the proportionality factor $K_{f,i}$. This proportionality factor is dependent on the geometry of the screw element.

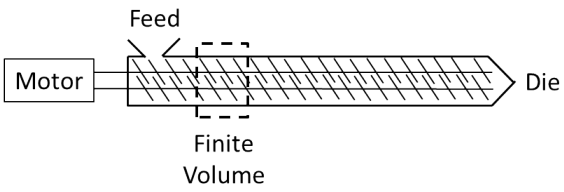

Fig. 1. Schematic of the modelled system.

This formulation of the internal conveying flow was first proposed by Kohlgrüber (2008) and further developed by Eitzlmayr et al. (2013) and Eitzlmayr et al. (2014). Depending on the orientation of the screw elements, the screw is pushing the material forward in the direction towards the die or backwards. The conveying flows can be quantitatively described by:

$$\dot{m}_{c,i} = \rho \cdot f_i \cdot K_{f,i} \cdot n \cdot D^3. \tag{1}$$

The second flow phenomena is the pressure induced flow $m_{p,i}$ which occurs if in an entirely filled element a pressure p_i has built up. The pressure flow is a function of the pressure drop Δp_i, the dynamic viscosity η_i, the diameter D and the proportionality factor $K_{p,i}$ that is dependent on the screw geometry. The pressure flow that moves the material in the direction opposite to the pressure gradient is described by:

$$\dot{m}_{p,i} = \rho \cdot K_{p,i} \frac{D^4}{\eta_i} \cdot \frac{\Delta p_i}{\Delta x}. \tag{2}$$

The evolution of the filling ratio f within a section of volume V_i of the extruder with the conveying flow can be described as:

$$\frac{\partial f_i}{\partial t} = \frac{1}{\rho_i V_i}\left(\dot{m}_{in,i} - \dot{m}_{out,i}\right). \tag{3}$$

The dynamics of the filling ratio for a fully filled element which has a pressure build-up are given by:

$$\frac{\partial f_i}{\partial t} = 0. \tag{4}$$

The switching of the dynamics is realized by branching during the simulation.

2.2 Pressure model

Choulak et al. (2004) and Eitzlmayr et al. (2014) suggested the calculation of the pressure in the elements by the solution of a system of linear equations to fulfill the internal mass-balance of the completely filled elements. Then the pressure along the reactor is described by:

$$\overline{\mathrm{A}} \cdot \overline{\mathrm{x}} = \overline{\mathrm{b}}. \tag{5}$$

The right-hand side $\overline{\mathrm{b}}$ is accounting for the violation of the mass balance. The matrix $\overline{\mathrm{A}}$ is a band matrix that contains the pressure flow proportionality factors of the individual elements. The dimension of the pressure vector $\overline{\mathrm{x}}$ corresponds to the number of completely filled elements with $f = 1$. As the locations of the completely filled zones change dynamically, the structure of the equation has to be adjusted over time. This creates problems for the use of efficient gradient based optimization methods in solving the dynamic optimization problems in MPC. Therefore, in contrast to the previous work, we suggest the application of a singular perturbation approach and introduce the calculation of the pressure within the section as a differential state. This state fulfills the mass balance with very fast dynamics by adjusting the pressure in each section.

$$\begin{aligned}\frac{\partial p_i}{\partial t} = c\frac{1}{\rho_i V_i}\big(\ & \dot{m}_{f,i-1} + \dot{m}_{b,i+1} + \dot{m}_{p,i-1} \\ & -\dot{m}_{p,i} - \dot{m}_{f,i} - \dot{m}_{b,i}\big)\end{aligned} \tag{6}$$

The drawback of the method is the introduction of very fast dynamics. The choice of the pressure dynamic constant c is determined by two factors: in case of a too small value of the dynamic pressure constant, the violation of the mass balance is the dominating effect. An increase of the constant results in an increasing stiffness of the system of differential equations causing numerical problems for the integrator. The major advantage however, is that the system of equations has the same structure for all operating modes and therefore standard non-linear solvers can be applied while a similar prediction accuracy for the pressure is maintained.

2.3 Temperature

The melt temperature T_m in each element is calculated by solving the local energy balance. The temperature has an influence on the viscosity and consequently on the dissipated mechanical energy Q_{diss} within the element. The melt has the specific heat capacity c_p. Heat transfer takes places between the barrel and the melt, described by Q_{bm}. The reaction is introducing the energy $Q_{reaction}$ into the system, as each reacted mole monomer releases the heat of reaction - ΔH. The temperature balance for the melt is:

$$\begin{aligned}\frac{\partial T_{m,i}}{\partial t} = & \frac{1}{\rho_i V_i c_p f}\big(\dot{Q}_{bm} + \dot{Q}_{diss} + \dot{Q}_{react} \\ & + \sum T_{m,i} \cdot \dot{m}_i \cdot c_{p,i}\big) - \frac{\partial f}{\partial t} \cdot \frac{T_{m,i}}{f_i}.\end{aligned} \tag{7}$$

The barrel temperatures are assumed as constant within a section as it is mostly the case in practice. For these sections the temperature set-points are regulated by electrical heating rods and cooling water which are controlled by internal PID controllers. A significant improvement of the performance by advanced process control cannot be expected due to the very slow dynamics of the barrel elements caused by the high thermal capacity of the steel blocks and the limited actuation. The heat transfer coefficient between barrel and melt is calculated by the empirical correlation developed by Tenge and Mewes (2000) between the Nusselt (Nu) and Brinkmann number (Br):

$$Nu = 2.9 Br^{0.8}. \tag{8}$$

2.4 Reaction System

The ring-opening polymerization of ϵ-Caprolactone is initiated by titanium propoxide. Commonly for polymerization processes, the initiator concentration is important for the final product quality as with increasing initiator concentrations the final product consists of a higher number of

shorter polymers chains with a lower molecular weight. Therefore the initiator concentration I is considered as an internal state as it not only influences the reaction rate but also has a direct influence on the rheology of the melt. The component balances are solved as differential equations connecting the internal flows with the corresponding concentrations over the length of the extruder. The reaction system is modeled as described by Dubois et al. (1996). The parameters of the model are shown in Tab. 1. The change in the monomer concentration M depends on the activation energy E_a,the temperature T and the universal gas constant R and the initiator concentration I and can be described by:

$$\frac{d[M]}{dt} = -1.2 \cdot 10^{16} \cdot [M] \cdot [I]^{\alpha} \exp\big(\frac{-E_a}{RT}\big). \tag{9}$$

The relationship between the weight average molecular weight M_w, the conversion X and the initial monomer concentration M_0 is as proposed by Gimenez et al. (2000):

$$M_w = X(39 \cdot M_0/I + 79) + 114. \tag{10}$$

The rheology of this system can be described by a generalized Cross-Carreau equation following Gimenez et al. (2000). The zero shear viscosity η_0 with the activation energy E_V can be described as:

$$\eta_0 = 1.35 \cdot 10^{-17} \cdot \exp\big(\frac{E_v}{R}\big(\frac{1}{T} - \frac{1}{T_0}\big)\big) \cdot M_w^{4.1}. \tag{11}$$

The viscosity at the shear rate $\dot{\gamma}$ with the pseudoplastic index a and the power index n is given as:

$$\eta(\dot{\gamma}) = \frac{\eta_0}{\big[1 + (\tau \cdot \dot{\gamma})^a\big]^{(1-n)/a}}. \tag{12}$$

The relaxation time τ is defined as:

$$\tau = 1.7 \cdot 10^{-20} \exp\big(\frac{E_v}{R}\big(\frac{1}{T} - \frac{1}{T_0}\big) \cdot M_w^{4.1}. \tag{13}$$

Table 1. Parameters for the reaction and the rheology model [Gimenez et al. (2000),Dubois et al. (1996)].

parameter	value	unit
ΔH	-250	J/g
M_0	10.61	mol/L
ρ	1210	kg/m^3
E_a	92600	kJ/mol
E_V	40000	kJ/mol
R	8.314	J/mol K
T_0	120	^{o}C
α	3.25	-
n	0.52	-
a	1.25	-

3. SIMULATION STUDIES

The reactive process is simulated for a Leistritz LSM 30-34 extruder with a screw diameter of 34 mm, a centerline distance of 30 mm , a barrel diameter of 38 mm and a total length of 1.2 m. The die is a round die with a diameter of 10 mm and a length of 40 mm. The screw geometry consists of simple double flighted conveying screw elements with a pitch of 24 mm. The extruder was discretized in 31 elements. The model was solved using

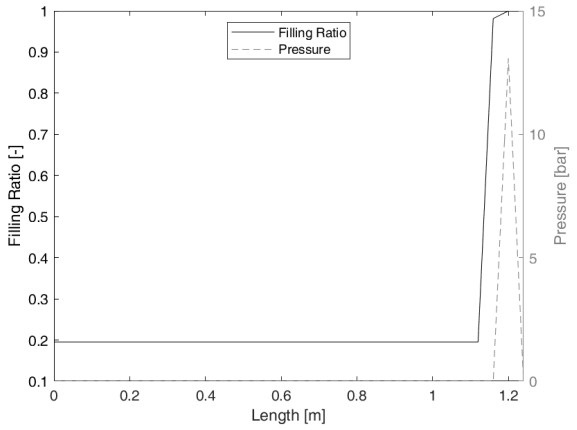

Fig. 2. Simulation of the filling ratio and the local pressures for a throughput of 20 kg/h, 100 rpm and a barrel temperature of 125 ^{o}C.

CasADI [Andersson et al. (2019)] and the integrator IDAS. Fig. 2 shows the simulation results for a throughput of 20 kg/h, a barrel temperature of 125 ^{o}C, a rotation speed of 100 rpm and a monomer to initiator ratio of 1000. The feed is injected molten at a temperature of 120 ^{o}C. The simulation results show the constant filling ratio of 0.2 due to the screw type for the first section of the extruder. For the last 10 cm a back-pressure zones builds up with an almost linear pressure increase. The deviation from a linear profile can be explained by the pressure flows that are a function of the locally varying temperature and conversion. The temperature and conversion profiles are shown in Fig. 3. Initially the melt is heated up from

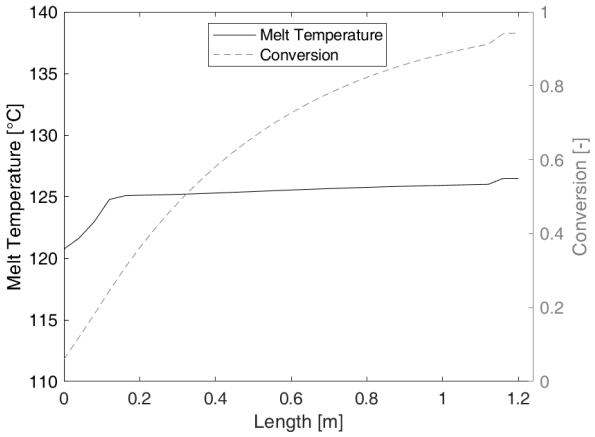

Fig. 3. Simulation of the melt temperature and the conversion for a throughput of 20 kg/h, 100 rpm and a barrel temperature of 125 ^{o}C

the feed temperature to the barrel temperature and the temperature then is maintained at the barrel temperature. This is a result of the high heat transfer between the barrel and the melt. The conversion rate over the length of the extruder decreases due to the decrease of the monomer concentration causing a lower reaction rate. Within the pressurized zone, the conversion rate increases due to the larger residence time of the melt in this zone caused by the larger filling ratio. The two main contributors to the heat balance are the mechanical heat dissipation that increases

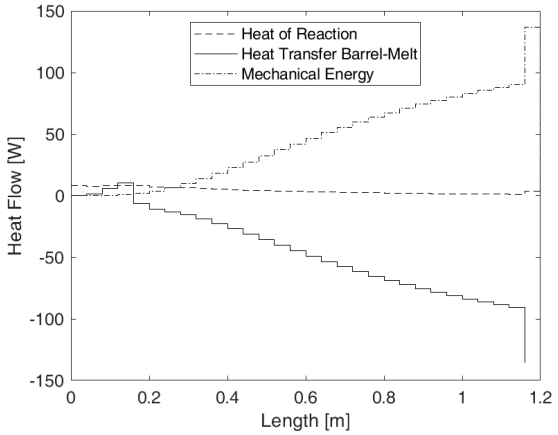

Fig. 4. Different contributions to the heat balance of the melt over the length of the extruder.

due to the higher viscosity at higher conversions and higher molecular weights and the heat removal by the barrel. The heat generated by the reaction is insignificant for this reaction system. Fig. 4 shows the evolution of these different contributions over the length of the extruder. Towards the die, the mechanical dissipation of energy increases. The heat transfer between the melt and the barrel is sufficient to remove the dissipated energy. In the process the viscosity increases from 5 Pas to 15000 Pas.

4. CONTROL AND OPTIMIZATION

4.1 Pressure control

The most obvious control objective in this system is to control the pressure at the extruder die. This pressure is directly measurable by a pressure probe and can be used for the calculation of the weight average molecular weight of the polymer, the main product quality criterion. For the given process, pressure control with traditional methods such as PI and PID controllers is unsuitable [Broadhead et al. (1996)]. Reasons for this are the long time delays in the process which are caused by the mass transport. Gimenez et al. (2000) proposed the application of internal model control for this process to compensate this effect. For this method it is necessary to perform system identification for a fixed set of processing parameters (throughput, rotation speed and barrel temperature). The resulting second order model plus dead time for the residence time of the melt in the extruder was then used in the internal model process control scheme to drive the process to the desired pressure set-point by varying the initiator to monomer ratio. As proposed already by Grimard et al. (2016) for a blending process with a much simpler model, NMPC can be successfully applied to twin-screw extrusion systems. The general optimization problem for MPC can be formulated as:

$$\min_{u_k \ldots u_k+N_C} J(t_k) \tag{14}$$

$$s.t.\ \ \dot{x} = f(f, p, T_m, X, I) \tag{15}$$

$$y = Cx \tag{16}$$

$$u_{min} \leq u \leq u_{max}, \tag{17}$$

with the inputs u applied during the interval k, the length of the control horizon N_C and the state vector x. Full state feedback is assumed. The cost function $\mathrm{J}(t_k)$ is based on the quadratic deviation of the state vector from the reference x_{ref}. Furthermore the changes of the inputs are penalized and weighted by a parameter λ. The cost function then results as:

$$J(t_k) = \sum_{i=1}^{N_p}((x_{k+i} - x_{ref})^2 + \lambda \sum_{i=1}^{N_C}(\Delta u_{k+i})^2. \tag{18}$$

The optimization problem is solved using IPOPT Wächter and Biegler (2006) using direct single shooting.

4.2 Change of the Product Quality

A plausible control target in the operation of a reactive extrusion system is a planned change of the pressure at the die which corresponds to a product changeover. The monomer to initiator ratio of the feed has a strong influence on the final molecular weight and on the pressure. The step response of the system from a monomer to initiator ratio of 1000 to 900 is depicted in Fig. 5. It clearly shows the time delay of the system of about 60 s, mainly caused by the transport delay within the extruder. Fig. 6 shows the influence of the speed of rotation

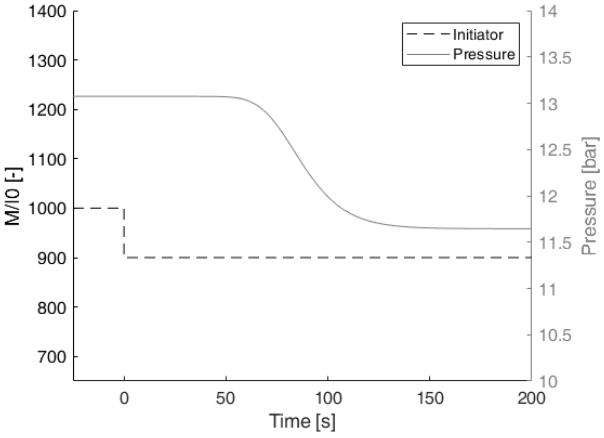

Fig. 5. Step response of the die pressure to an input step on the monomer to initiator ratio M/I0 from 1000 to 900.

on the residence time distribution. The mean residence time at 100 rpm is about 80 seconds. With increasing speed of rotation, the residence time decreases since the filling ratio increases over the length of the extruder. As the screw in the example consists only of conveying elements, the behavior of the reactor is close to a pure plug flow with only little back-mixing caused by the fully filled pressurized zones at the end of the extruder. This is in accordance with the investigation of Puaux et al. (2000) of the residence time distribution within twin-screw extruders. Changes that result in a higher pressure at the die increase the fully filled back-pressure zone and therefore increase the residence time. Controllers that do not include these effects have a poor performance since these effects strongly affect the response of the system. Therefore the application of model predictive control is promising. The optimized input is the monomer to initiator ratio in the range of 700 to 1300 for which the model is valid. The penalty on the input changes λ is

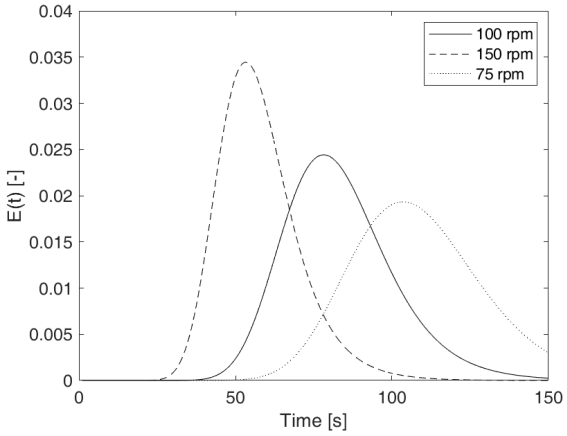

Fig. 6. Residence time distribution of the extruder for a throughput of 20 kg/h for different rotation speeds.

fixed throughout to the value of 10^{-6}. Simulations show that an increased penalty results in a better damped but also slower solution. The optimal trade-off depends on the characteristics of the real actuator. Simulations with different lengths of the prediction and control horizons are shown in Fig. 7 for a sampling time of 30 seconds. The tracking objective of the controller is to realize a

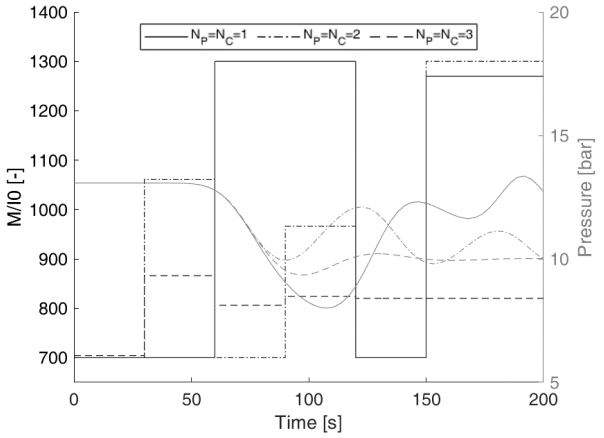

Fig. 7. Results of the application of MPC for different values of $N_c = N_p$ for a pressure change to 10bar.

pressure at the die of 10 bar. The results show that with a control horizon for $N_C = N_P = 1$, the controller is unable to drive the process to the desired set-point as the prediction horizon is shorter than the residence time. For $N_C = N_P = 2$, the influence of the changes in the monomer to initiator ratio is only included partially. For $N_C = N_P \geq 3$, the controller is capable of driving the process to the desired set-point within two residence times. Comparing this results to the application of internal-model control proposed by Gimenez et al. (2000), this is a reduction of the time to reach the target by 50% as their method requires at least four residence times to converge to the target. Simulations with different lengths of the prediction horizon with a control horizon of $N_C = 1$ are shown in Fig. 8. The performance with a prediction horizon of $N_P = 2$ is comparable to the performance of a control horizon of $N_C = N_P = 2$. A prediction horizon of $N_P = 4$ results in the best performance as the combination of prediction and control horizon exceeds the residence time. Further increase of the prediction horizon decreases the performance of the controller, as the steady-state response of the control inputs is weighted higher than the transient response. The computation time per step is about 100 s (Intel Core i7-7700).

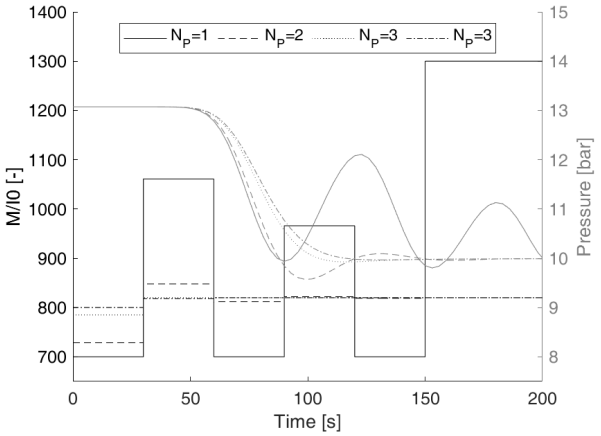

Fig. 8. Results of the application of MPC for different N_p for N_c=1 for a pressure change to 10bar.

4.3 Change of the Throughput

The second relevant control scenario is a change of the throughput of the extruder while maintaining the product quality. To investigate the dynamics of the system, the system is initialized at steady state operating conditions. Then the throughput of the system is increased. The control objective is the tracking of the desired pressure set-point. Without control action one would observe an inverse response and an overshoot of the pressure that leads to the production of off-spec product (Fig. 9). The

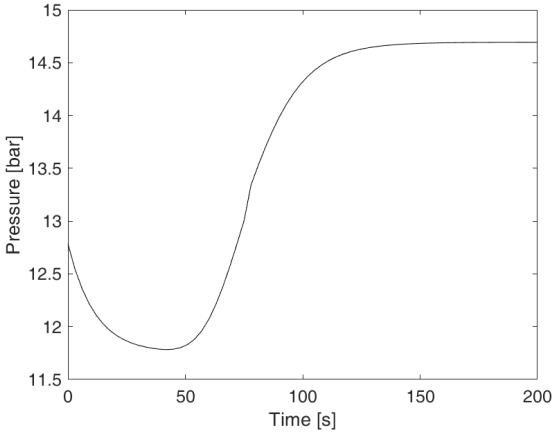

Fig. 9. Step response of the system to an increase of the throughput from 20 kg/h to 25 kg/h

inverse response results because the increased throughput causes a higher shear rate. The results of the application of nonlinear model predictive control to this case with a control and prediction horizon of 120 seconds (4 steps) are shown in Fig. 10. For PID control or internal model

control the performance for this case is very poor as both require multiple residence times to react to the change in the throughput. Applying model predictive control, it is possible to move the process to the desired set-point after only two residence times. This performance can be furthermore improved by supplying the MPC with the information on the set-point change ahead of time.

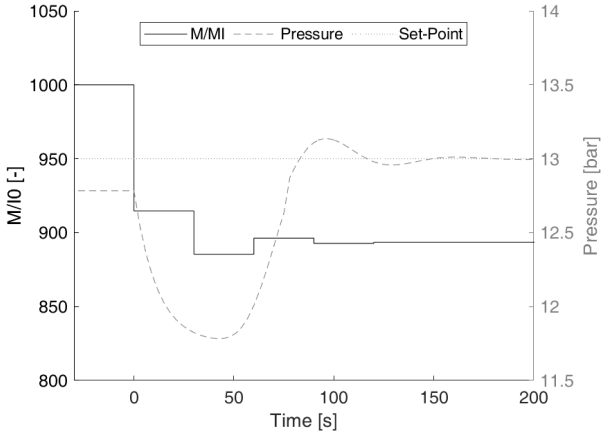

Fig. 10. Results of MPC pressure control after a throughput change from 20 kg/h to 25 kg/h at 0 s.

4.4 Conclusions

The application of model predictive control shows a very promising performance for both investigated cases. The use of the information from the process model is a major benefit of this method making it applicable to a very wide range of operating conditions. Tuning of the method requires sufficiently long prediction horizons. The optimal choice for the penalty on the input change λ depends on the technical realization of the actuators. Furthermore constraints such as maximum temperatures can be taken into account for cases where product degradation occurs.

5. SUMMARY AND OUTLOOK

This paper presented the modeling of a reactive extrusion system in a twin-screw extruder and its control using nonlinear model predictive control. In both scenarios of changes of the product quality and the adjustment after a throughput change show benefits over traditional control methods. For a real online application of the controller , the computation time must be reduced to about 1/4 and the control scheme must be extended by a state estimator. Reduction of the computation time is possible using a broader discretization of the model or a more efficient problem formulation with tools like do-mpc [Lucia et al. (2017)]. The developed model enables the economic optimization of the process not only with respect to the operational parameters but as well for the design parameters such as machine size and screw setup.

ACKNOWLEDGEMENTS

This work has received funding from the European Union's Horizon 2020 research and innovation programme under grant agreement No 820716 (SIMPLIFY).
(www.spire2030.eu/simplify)

REFERENCES

Andersson, J.A., Gillis, J., Horn, G., Rawlings, J.B., and Diehl, M. (2019). CasADi: a software framework for nonlinear optimization and optimal control. *Mathematical Programming Computation*, 11(1). doi:10.1007/s12532-018-0139-4.

Broadhead, T.O., Patterson, W.I., and Dealy, J.M. (1996). Closed loop viscosity control of reactive extrusion with an in-line rheometer. *Polymer Engineering and Science*, 36(23), 2840–2851. doi:10.1002/pen.10685.

Choulak, S., Couenne, F., Le Gorrec, Y., Jallut, C., Cassagnau, P., and Michel, A. (2004). Generic dynamic model for simulation and control of reactive extrusion. *Industrial and Engineering Chemistry Research*, 43(23), 7373–7382. doi:10.1021/ie0342964.

Dubois, P., Ropson, N., Jérôme, R., and Teyssié, P. (1996). Kinetics of ring-opening polymerization of ϵ-caprolactone initiated with functional aluminum alkoxides. *Macromolecules*, 29(6), 1965–1975. doi:10.1021/ma951738h.

Eitzlmayr, A., Khinast, J., Hörl, G., Koscher, G., Reynolds, G., Huang, Z., Booth, J., and Shering, P. (2013). Experimental characterization and modeling of twin-screw extruder elements for pharmaceutical hot melt extrusion. *AIChE Journal*, 59(11), 4440–4450. doi:10.1002/aic.14184.

Eitzlmayr, A., Koscher, G., Reynolds, G., Huang, Z., Booth, J., Shering, P., and Khinast, J. (2014). Mechanistic modeling of modular co-rotating twin-screw extruders. *International Journal of Pharmaceutics*, 474(1-2), 157–176. doi:10.1016/j.ijpharm.2014.08.005.

Gimenez, J., Boudris, M., Cassagnau, P., and Michel, A. (2000). Control of bulk ϵ-caprolactone polymerization in a twin screw extruder. *Polymer Reaction Engineering*, 8(2), 135–157. doi:10.1080/10543414.2000.10744545.

Grimard, J., Dewasme, L., and Vande Wouwer, A. (2016). Nonlinear model predictive control of a twin-screw extruder. *SINTES 20, SACCS 16, SIMSIS 20 - Proceedings*, 46(1), 204–209. doi:10.1109/ICSTCC.2016.7790666.

Kohlgrüber, K. (2008). *Co-Rotating Twin-Screw Extruder Fundamentals, Technology, and Applications*. Carl Hanser Verlag GmbH & Co. KG, Munich.

Lucia, S., Tătulea-Codrean, A., Schoppmeyer, C., and Engell, S. (2017). Rapid development of modular and sustainable nonlinear model predictive control solutions. *Control Engineering Practice*, 60, 51–62. doi:10.1016/j.conengprac.2016.12.009.

Puaux, J., Bozga, G., and Ainser, A. (2000). Residence time distribution in a corotating twin-screw extruder. *Chemical Engineering Science*, 55(9), 1641–1651. doi:10.1016/S0009-2509(99)00430-3.

Tenge, S. and Mewes, D. (2000). Experimental investigation of the energy balance for the metering zone of a twin screw extruder. *Polymer Engineering and Science*, 40(2), 277–289. doi:10.1002/pen.11161.

Wächter, A. and Biegler, L.T. (2006). On the implementation of an interior-point filter line-search algorithm for large-scale nonlinear programming. *Mathematical Programming*, 106(1), 25–57. doi:10.1007/s10107-004-0559-y.